RESEARCH LETTER

Key Points:

- We report the first evaluations of frictional stability properties for laumontite gouge and mixtures under hydrothermal conditions
- Gouges are strongly velocity-weakening over a broad range of temperatures and insensitive to pressures and relative proportions
- This instability field is coincident with P-T conditions typical for EGS and hence an indicator of ubiquitous seismic hazard

Supporting Information:

Supporting Information may be found in the online version of this article.

Correspondence to:

C. Zhang,
zhchongyuan@126.com;
zhangchy@cags.ac.cn

Author Contributions:

Conceptualization: Chongyuan Zhang, Manchao He
Data curation: Zijuan Hu
Formal analysis: Chongyuan Zhang, Zijuan Hu, Derek Elsworth, Lei Zhang, Hao Zhang, Manchao He, Leihua Yao
Investigation: Zijuan Hu, Hao Zhang, Linyou Zhang
Methodology: Chongyuan Zhang, Zijuan Hu, Lei Zhang
Software: Lei Zhang

Frictional Stability of Laumontite Under Hydrothermal Conditions and Implications for Injection-Induced Seismicity in the Gonghe Geothermal Reservoir, Northwest China

Chongyuan Zhang[1,2,3] , Zijuan Hu[1,4], Derek Elsworth[5,6] , Lei Zhang[7] , Hao Zhang[1,3], Linyou Zhang[8], Manchao He[2], and Leihua Yao[4]

[1]Institute of Geomechanics, Chinese Academy of Geological Sciences, Beijing, China, [2]School of Mechanics and Civil Engineering, China University of Mining and Technology, Beijing, China, [3]Technology Innovation Center for In-situ Stress, Ministry of Natural Resources, Beijing, China, [4]School of Engineering and Technology, China University of Geosciences (Beijing), Beijing, China, [5]Department of Energy and Mineral Engineering, EMS Energy Institute and G3 Center, The Pennsylvania State University, State College, PA, USA, [6]Department of Geosciences, The Pennsylvania State University, State College, PA, USA, [7]State Key Laboratory of Earthquake Dynamics, Institute of Geology, China Earthquake Administration, Beijing, China, [8]Center for Hydrogeology and Environmental Geology Survey, China Geological Survey, Baoding, China

Abstract Laumontite is a common and potentially frictionally unstable hydrothermal alteration product present in deep faults of the Gonghe EGS reservoir. We characterize the friction-stability characteristics of synthetic laumontite gouge under in situ reservoir conditions. The pure laumontite gouge is frictionally strong ($\mu = 0.73$–0.98) and the quartz/laumontite mixture (1:1) is generally less strong ($\mu = 0.73$–0.78) under experimental conditions ($P_c = 95$ MPa, $T = 90$–$250°C$, $P_f = 0$–90 MPa). The shear velocity was stepped between 6.1, 0.61, then 0.061 μm/s for our experiments. For both gouges, the friction coefficient is independent of temperature and increases with elevated pore pressures. The pure gouge and mixture are strongly velocity-weakening over a broad range in temperatures ($\sim$90–220°C) and excess pore pressures (0–90 MPa) relevant to the Gonghe stimulation. Microearthquakes (MEQs) observed during stimulation are confined to within the broad depth range of inferred frictional instability—although fluid overpressures are also limited to this region. The observation that laumontite mixtures are frictionally unstable over a broad range of pressures and especially temperatures representative of EGS reservoirs and insensitive to the presence of the coexisting mineral phase (quartz) suggests its presence is a strong indicator of potential seismic hazard.

Plain Language Summary Laumontite is a very low-grade altered mineral that can easily occur in fractures or faults in granite, basalt, or sandstone. Laumontite is widely developed in the Gonghe geothermal reservoir of Western China. Fluid injection into deep geothermal rock mass may reactivate subsurface faults containing altered minerals and cause earthquakes. Hence, we conducted laboratory experimental analysis on the frictional characteristics of simulated laumontite gouge to further understand the impact of fluid injection on the triggering of deep fault earthquakes. These experiments were performed at conditions reflecting the temperature and pressure of the water injection depth of the Gonghe geothermal reservoir. The results showed that the fault's strength and friction stability strongly depend on pore pressure and temperature. Our study emphasizes the significant role of the altered mineral laumontite in controlling fault strength and stability, as well as its potential for inducing earthquakes. A possible implication of this work is that when selecting geothermal resource targets that require fluid-injection operations, it is best to avoid laumontite-rich sites or reservoir sections.

1. Introduction

Induced seismicity has become a major hazard in the recovery of unconventional resources, including enhanced geothermal systems (EGS), and shale gas reservoirs (Ellsworth, 2013; Igonin et al., 2021; Majer et al., 2007). Injection of overpressured fluids has triggered fault reactivation and induced earthquakes (Bao & Eaton, 2016; Hubbert & Rubey, 1959; Schultz et al., 2018). Such hazards can only be mitigated if frictional and stability properties are suitably defined (Ikari et al., 2011; Logan & Rauenzahn, 1987; Niemeijer & Collettini, 2014; Shimamoto & Logan, 1981).

Validation: Chongyuan Zhang,
Derek Elsworth
Visualization: Chongyuan Zhang,
Derek Elsworth
Writing – original draft:
Chongyuan Zhang, Zijuan Hu,
Derek Elsworth, Lei Zhang, Manchao He
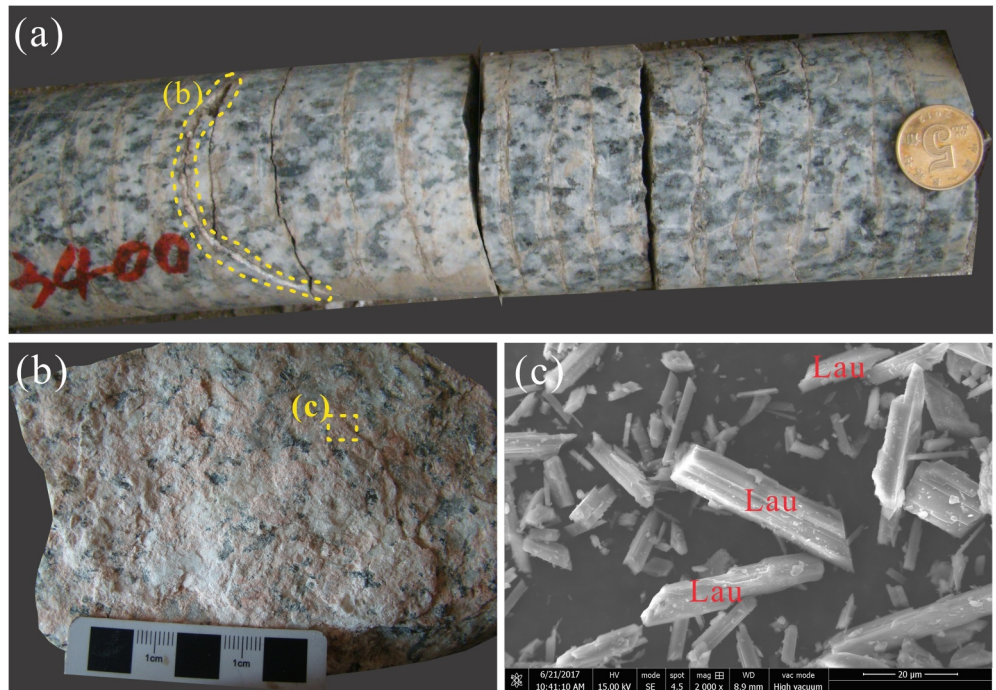**Writing – review & editing:** Hao Zhang

Figure 1. Photographs of (a, b) granite rocks recovered from ∼3.4 km depth of the Gonghe EGS reservoir in Western China and (c) backscattered electron SEM (scanning electron microscopy) images of laumontite mineral. The surface of natural fractures is coated with many ∼1–2 mm thick, pink laumontite films (b). The areas without film-covered are due to the detachment of unconsolidated laumontite powder when the filled fracture is opened.

The Gonghe Basin, located on the northeastern margin of the Tibetan Plateau in China, possesses abundant and high-quality geothermal resources (E. Zhang et al., 2022). Like most granite geothermal reservoirs, abundant altered minerals were inspected in the fractured cores retrieved from the Gonghe reservoir—laumontite exists as a very-low-grade mineral phase in this granitic hydrothermal system (Figure 1). In 2020–2022, tens of thousands of cubic meters of water were injected into the Indosinian granite reservoir in five stages, triggering many MEQs (including some felt events) (Text S1, Figures S1 and S2 in Supporting Information S1). Considering the active seismic potential and high-stress levels around the Gonghe Basin, the stability of faults in the vicinity of the reservoir under hydraulic fracturing and injection circulation deserves attention. Hydrothermal alteration products present in gouges on mature faults that transect reservoirs are one critical factor controlling the frictional sliding and stability of faults (Okamoto et al., 2019). Low- and mid-grade metamorphism is common in granite reservoirs with common reaction products such as chlorite, epidote, and laumontite minerals (Bird & Spieler, 2004; Liou, 1993; Morrow et al., 2000; Okamoto et al., 2019). Of these, pure chlorite is generally frictionally weak (<0.5), and velocity-strengthening under hydrothermal conditions (Belzer & French, 2022; Ikari et al., 2009; Okamoto et al., 2019, 2020; Shimamoto & Logan, 1981; Smith et al., 2017). Conversely, pure epidote is mainly velocity-weakening under hydrothermal conditions (An et al., 2021; Fagereng & Ikari, 2020; Prante & Evans, 2015) with chlorite-epidote mixtures assuming intermediate characteristics aligned with their proportions (An et al., 2021). However, the properties of laumontite remain poorly constrained under hydrothermal conditions of interest.

Laumontite ($Ca_2[AlSi_2O_6]_2 \cdot 4H_2O$) is a framework aluminosilicate mineral composed of $(Si/Al) O_4$ tetrahedral rings, which is commonly found in geosynclinal sediments and thicker sequences of igneous rock (Heidari et al., 2023; Liou, 1971a). Laumontite is mineralogically stable over 90–220°C but dehydrates >220°C, where its frictional properties may change (Morrow & Byerlee, 1991; Morrow et al., 2000). To date, few laboratory studies define the frictional strength of laumontite gouges under hydrothermal conditions (Morrow & Byerlee, 1991; Morrow et al., 2000) and none define stability characteristics. Frictional strengths ($\mu \sim 0.66$–0.84; Cajon Pass, San Andreas fault) are generally much higher than clay-rich gouges ($\mu \sim 0.3$) (James & Silver, 1988; Morrow & Byerlee, 1991) with frictional stability undefined. Previous studies showed that the metamorphic reaction of

the stilbite produces laumontites, quartz, and water, thus laumontite often coexists with quartz (stilbite = laumontite + 3 quartz + 3 H_2O, Liou, 1971b). Laumontite is broadly present with quartz in retrieved cores from the Gonghe EGS field, China (S. Zhang et al., 2018; Figure 1) and presents an unknown impact on fault stability and the potential for seismicity. Therefore, the friction characteristics of the mixture of laumontite and quartz in geothermal systems under the influence of anthropogenic fluid-injection activities are also worth exploring. We report the results of shear-reactivation experiments on synthetic mixed fault gouges (50% laumontite and 50% quartz) representative of conditions at 3.7 km for hydraulic stimulation in the Gonghe EGS reservoir.

2. Material and Methods

We collected laumontite and quartz minerals powders from Xinzhou City of Shanxi Province, China. After removing impurities, the laumontite and quartz samples were crushed and sieved to <75 μm to simulate gouge. The median particle sizes of the laumontite (12.7 μm) and quartz (35.3 μm) (Figure S3 in Supporting Information S1) are defined by laser classifier. X-ray diffraction indicates that both the laumontite and quartz gouges have >99 wt.% purity (Figure S4 in Supporting Information S1). The mixed gouge used in the experiments was prepared by homogeneously mixing laumontite and quartz 1:1 by weight.

The thin (1 mm) gouge samples are jacketed between angled gabbro forcing blocks (Text S3 in Supporting Information S1) and sheared under confining stress (P_c) of 95 MPa and pore pressure (P_f) of 35 MPa corresponding to lithostatic and hydrostatic conditions (rock density of 2,630 kg/m^3) at 3.7 km in the Gonghe geothermal reservoir. Projected maximum pore pressures during stimulation are anticipated at ∼90 MPa. Thus, we examine frictional properties of the laumontite gouge at P_c = 95 MPa, T = 90–250°C, P_f = 0–90 MPa, and laumontite/quartz mixtures at P_c = 95 MPa, T = 180–220°C, P_f = 35–70 MPa (Tables S1 and S2 in Supporting Information S1). For the experiment of P_f = 0 MPa, the gouges are saturated with water, placed between upper and lower gabbro driving blocks, and then left at 250°C for 1 hr to dry. Each sample was initially sheared at a constant shear velocity (0.61 μm/s) to steady-state friction. Then, the shear velocity was stepped between 6.1, 0.61, then 0.061 μm/s to assess the velocity dependence and hence frictional stability of the gouge (see Text S3 in Supporting Information S1).

The raw data are corrected for the decrease in the nominal contact area of the simulated gouge layer with increasing axial displacement and for membrane restraint from the copper jacket with axial loading (for details see He et al., 2006, 2007; Text S2 in Supporting Information S1). The frictional coefficient μ of the simulated gouge is then defined as

$$\mu = \frac{\tau}{\sigma_{\text{neff}}} = \frac{\tau}{\left(\sigma_n - p_f\right)} \tag{1}$$

where τ is the corrected shear stress, σ_n is the corrected normal stress, and σ_{neff} is the effective normal stress.

Rate-dependent analysis of gouge friction is based on rate-state friction (RSF) theory (Dieterich, 1978, 1979a, 1979b; Marone, 1998; Ruina, 1983) as,

$$\mu = \mu^* + a\ln\left(\frac{V}{V^*}\right) + b\ln\left(\frac{V^*\theta}{D_c}\right) \tag{2}$$

$$\frac{d\theta}{dt} = 1 - \frac{V\theta}{D_c} - \frac{\alpha\theta}{b\sigma_{eff}}\frac{d\sigma_{eff}}{dt} \tag{3}$$

where μ is the frictional coefficient, μ^* represents the steady-state value of the frictional coefficient at the reference sliding rate V^*, a represents the direct effect characterizing frictional strength, V is the current loading rate, and b represents the evolutionary effect. The state variable θ evolves through the slowness law of Equation 3 where D_c is the characteristic sliding distance, α is a constant describing the effect of normal stress change, and σ_{eff} is the effective normal stress.
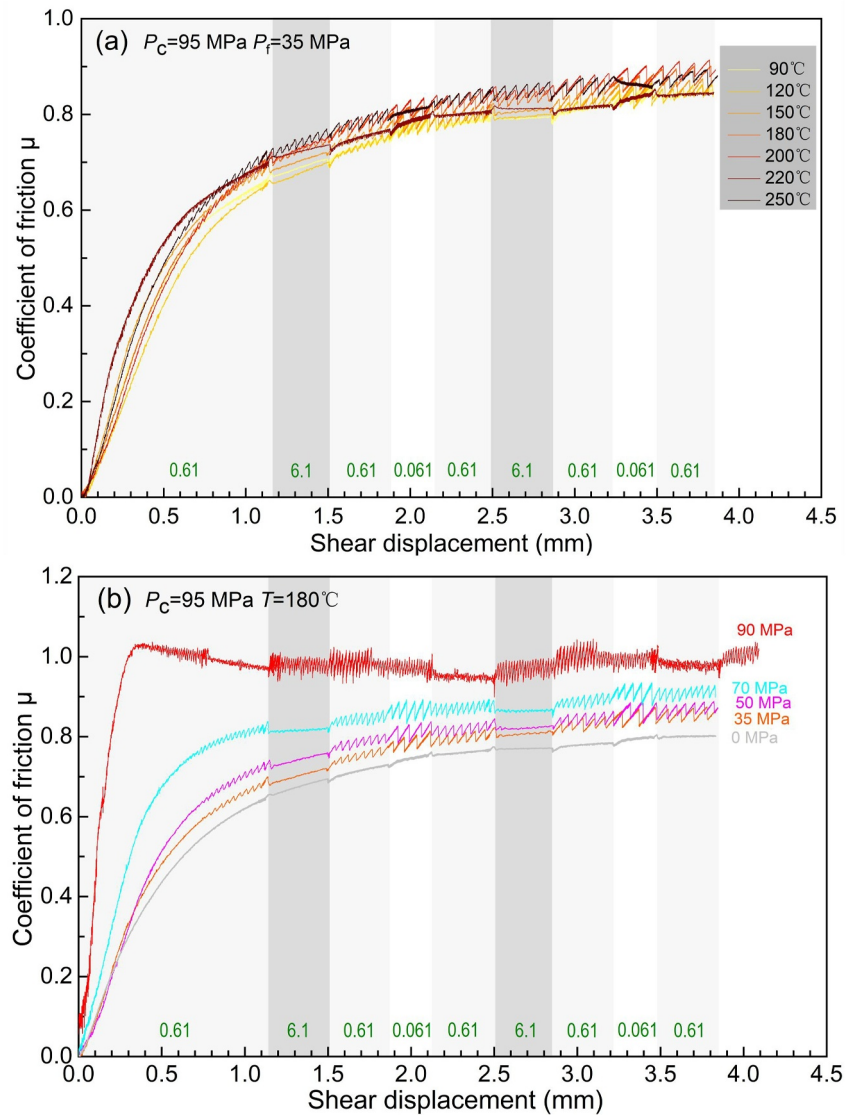
Figure 2. The friction-displacement curves for pure laumontite gouges under different experimental conditions. (a) P_c = 95 MPa and P_f = 35 MPa. (b) P_c = 95 MPa and T = 180°C.

When friction has evolved to a steady state, θ is invariant with time, thus $d\theta/dt = 0$, and the frictional coefficient is defined as,

$$\mu_{ss} = \mu^* + (a - b)\ln(V/V^*) \tag{4}$$

For quasi-static loading, when $a–b < 0$, the frictional coefficient decreases with increasing shear rate (velocity weakening) and the fault is conditionally unstable—with the potential for seismic nucleation. Conversely, when $a–b > 0$, the frictional coefficient increases with increasing rate (velocity strengthening) and the fault will fail stably without seismic sliding.

For stable sliding, parameter values for $a–b$ are recovered directly from the friction displacement curve. However, for quasi-static sliding (stick slips) data fitting is required. The specific fitting procedure is detailed in He et al. (2013).
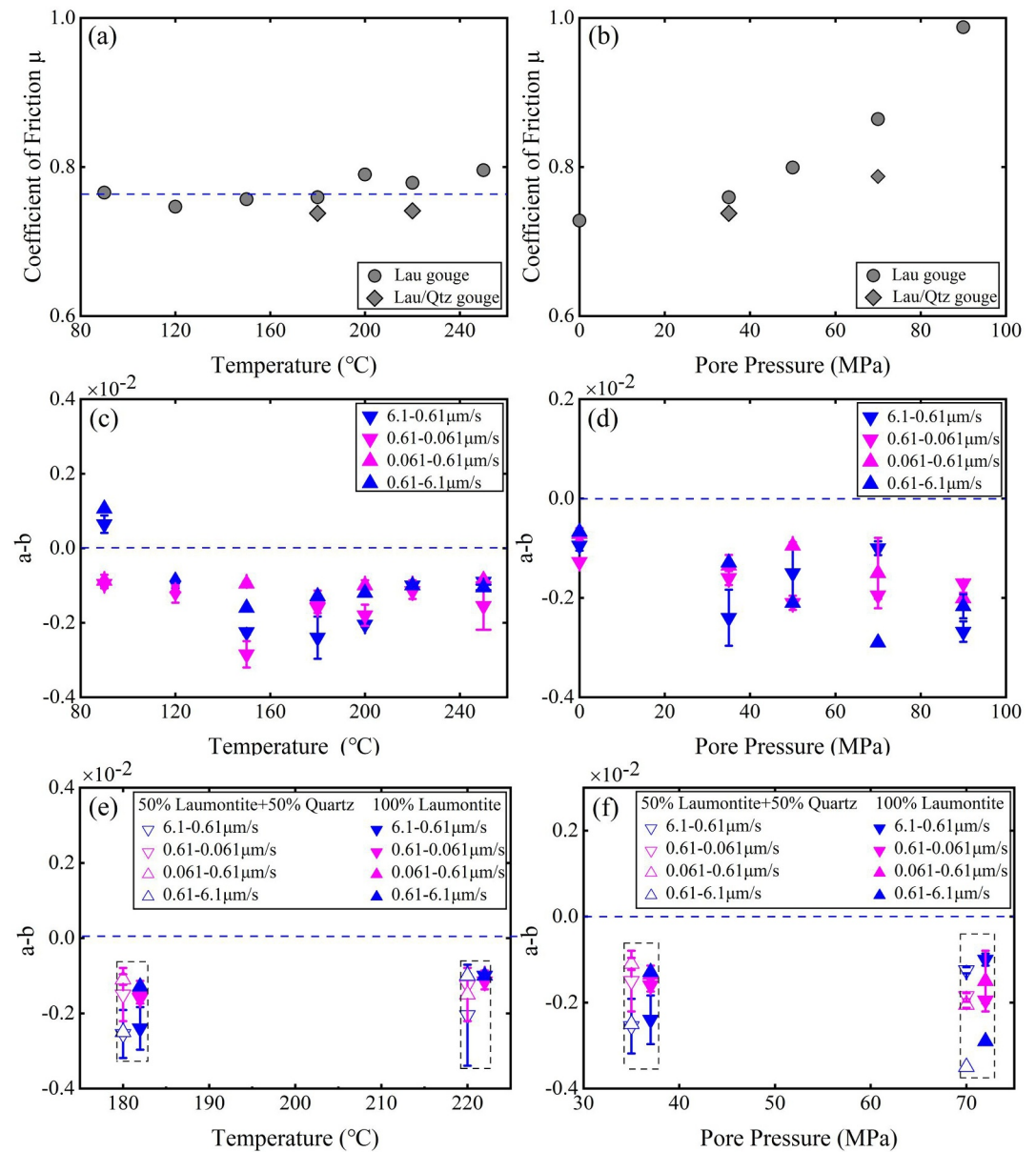
Figure 3. Coefficient of friction μ and frictional stability $a–b$ for laumontite (Lau) and laumontite/quartz (Qtz) mixed gouges at varied conditions. (a) Values of μ versus temperature of Lau gouge at $P_c = 95$ MPa and $P_f = 35$ MPa. The red dashed line indicates $\mu = 0.77$. (b) Relationship between frictional coefficient and pore pressure of Lau gouge at $P_c = 95$ MPa and $T = 180°C$. (c) $a–b$ as a function of temperatures of pure Lau gouge at $P_c = 95$ MPa and $P_f = 35$ MPa. (d) $a–b$ as a function of pore pressure of pure Lau gouge at $P_c = 95$ MPa and $T = 180°C$. (e) $a–b$ values of frictional stability coefficients of Lau/Qtz mixed gouges at $P_c = 95$ MPa, $T = 180°C$, $P_f = 35$ and 70 MPa; (f) $a–b$ values of frictional stability coefficients of Lau/Qtz mixed gouges. The plotted $a–b$ values are the average values from the same velocity steps in each test with the error calculated from the standard deviation (Table S2 in Supporting Information S1).

3. Results

Observations of the evolution of frictional coefficient with shear displacement were obtained (Figure 2; C. Zhang et al., 2023; Figures S8, and S9 in Supporting Information S1). Friction initially increases linearly during "running-in," followed by inelastic yielding and slip hardening. This slip hardening is apparent as the contact area and jacket correction might not be perfect. The laumontite gouge begins to show quasi-static oscillations when loaded at 0.061 μm/s at 120°C (Figure S8b in Supporting Information S1). Over our experimental temperature range (90–250°C), the frictional strength of the laumontite gouge was insensitive to temperature (Figure 3a) with

an average value is 0.76 (Table S2 in Supporting Information S1). The frictional strength of the gouge increased with the increase of pore pressure (Figure 3b) with μ values in the range 0.73–0.98 (Table S2 in Supporting Information S1). The frictional strength of the mixed laumontite/quartz fault gouge ($\mu = 0.73$–0.78) is lower than that of the laumontite gouge over the ranges of temperature (90–250°C) and pressure (0–90 MPa) of our experiments (Table S2 in Supporting Information S1).

The velocity dependence of the frictional strength during each velocity step is then analyzed by evaluating the values of the frictional stability parameter a-b (Figures 3c and 3d; Table S2 in Supporting Information S1). The pure laumontite gouge transitions from velocity-neutral (a–$b = -0.00096$ to 0.00106) at 90°C to velocity-weakening (a–$b = -0.00285$ to -0.00085) at $T \geq 120°C$. From 90°C to 180°C, a-b becomes progressively more negative with an increase in temperature before reversing this trend above 180°C and toward 250°C—but remaining negative and identifying an instability window. As pore pressure P_f increases from 0 MPa (a–$b = -0.00128$ to -0.00067) to 90 MPa (a–$b = -0.00268$ to -0.00170) the laumontite-rich faults exhibit conditional instability. The value of a–b decreases with increasing P_f for slow loading rates from 35 to 90 MPa (Figure 3d). The laumontite and laumontite/quartz mixed gouges are compared under different temperatures ($T = 180°C$, 220°C) and pore pressure conditions ($P_f = 35$ MPa, 70 MPa). Results show that both the pure laumontite and mixed gouges show velocity weakening behavior and over similar ranges of a–b (Figures 3e and 3f).

For RSF response, parameter a reflects the direct response of frictional strength to an instantaneous change in shear rate with the evolution toward a new steady state controlled by parameter b (He et al., 2013; Ruina, 1983). The distribution of frictional constitutive parameters a and b (Table S2 in Supporting Information S1) is shown in Figures S12a–S12d and S13a–S13d in Supporting Information S1. The characteristic slip distance D_c is an intrinsic parameter describing the completely evolved frictional response associated with the preseismic slip of mature faults with nucleation zones (Marone & Kilgore, 1993). As shown in Figures S12e and S12f in Supporting Information S1, Dc decreases with elevated pore pressure. The decrease in D_c increases the critical stiffness k_{cr} value and admits unstable sliding earlier for an evolving patch dimension (Dieterich, 1978, 1979a, 1979b; Rice, 1983; Ruina, 1983; Scholz, 1998). This is consistent with the quasi-static oscillatory behavior exhibited by laumontite in our range of test temperatures and pore pressures. The parameters a, b, and D_c and their inferred stability response change little as the laumontite content is reduced to 50% as quartz is substituted to the pure gouges (Figure S13 in Supporting Information S1).

Microstructural observations indicate that the local shear zones (LSZs) appear in the laumontite samples at experimental temperature and pressure, which are characterized by a significant reduction in particle size (Logan et al., 1992) (Figure 4; Figures S10, S11, and S13 in Supporting Information S1). The laumontite gouge is uniformly sheared over our range of test temperatures with multiple R_1 shears (Riedel Shear) observed throughout the gouge layers (Figure S10 in Supporting Information S1). Shear crushing in the local shear zone reduces most laumontite particles to <2 μm in diameter below the unchanged background particle size (~10 μm). At $P_f = 90$ MPa the R_1 shear was not apparent and the shear structure is featured by a boundary shear. More intense shear fragmentation of laumontite particles than quartz was observed in the mixed laumontite/quartz gouge samples—with laumontite grain sizes generally <1 μm and quartz particles in the range of 6–10 μm.

4. Discussion

4.1. Frictional Properties of Laumontite Gouge

Our frictional coefficient data for water-saturated laumontite (0.77 at $P_c = 95$ MPa and $P_f = 35$ MPa and $T = 90$–250°C (Figure 3a) are consistent with previous observations (0.6–0.8; James & Silver, 1988; Morrow & Byerlee, 1991; Morrow et al., 2000). Also, trends of frictional coefficient increasing with pore pressure at $T = 180°C$ (Figure 3b) are consistent with previous studies (Morrow & Byerlee, 1991). Significantly, the frictional coefficient of laumontite gouge exceeds unity at high pore pressures ($P_f = 90$ MPa; Figure S8h in Supporting Information S1) where the effective confining stress is correspondingly low (5 MPa). Under these conditions, the shear strength of the gouge is significantly impacted by its cohesive strength, with this impact minimal under higher effective stresses. This apparent cohesion in the initially disaggregated and cohesionless gouge is presumed to originate from compaction and then early geometric dilation at low normal effective stress.
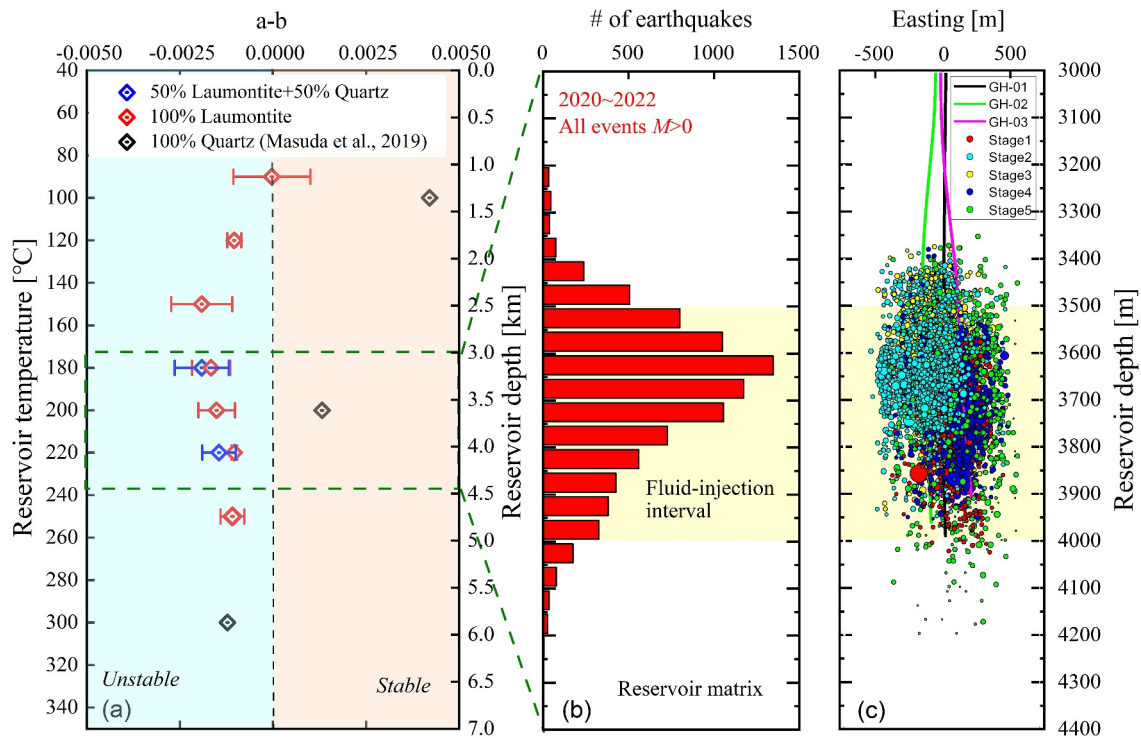
Figure 4. Depth dependency of frictional stability (a–b) of laumontite and quartz (a). The statistical (b) and spatial distribution (c) of MEQs during 5 stages of hydraulic fracturing stimulation in the Gonghe EGS in 2020–2022. The wells GH-01, GH-02, and GH-03 injected fluids into the reservoir at depths of ∼3,500–4,000 m (yellow ranges in (b, c)), respectively. All $M > 2$ events (maximum $M3.2$) are in the water injection zone. Note that (a–b) values are the average values from the all-velocity steps for different temperatures in our experiments with the error calculated from the standard deviation.

Temperature and pore pressure are key factors in affecting the stability of faults (Bedford et al., 2021; Blanpied et al., 1995; Chen et al., 2015; Chen & Spiers, 2016; C. Zhang et al., 2024). Fluid-mediated mass dissolution and redistribution (Chen & Spiers, 2016; Chen et al., 2015; den Hartog et al., 2012; Niemeijer & Spiers, 2007) with accelerated kinetics at higher temperatures explain velocity weakening behavior at elevated temperatures. This emphasizes the competition between dilation and dissolution-assisted compaction over a temperature transition, with resulting temperature-dependent frictional stability. In this study, our simulated laumontite gouge transitions from slight velocity strengthening at a larger slip rate of 6.1 μm/s at 90°C to complete velocity-weakening behavior across all tested slip rates at temperatures above 120°C(Chen & Spiers, 2016; Chen et al., 2015). This temperature dependent of the velocity dependence of gouge is mechanistically consistent with the microphysical CNS model (Chen & Spiers, 2016; Chen et al., 2015; den Hartog et al., 2012; Niemeijer & Spiers, 2007). Increasing temperature activates and enhances thermal-sensitive compaction processes (pressure solution or subcritical crack growth) that decrease porosity. The increasing trend of constitutive parameters a and b with temperature indicates the activation and enhancement of the thermally sensitive process in our gouge layer (Figure S12 in Supporting Information S1). However, according to our microstructure observation, no evident proof of pressure solution of laumontite can be found. Based on the rare experimental studies of laumontite, especially on its deformation mechanism map under P-T conditions, it is hard to conclude the background compaction processes incorporated into the CNS model to explain the temperature-dependent frictional stability.

At 180°C the laumontite gouge is velocity-weakening independent of pore pressure. This is an unequivocal and robust conclusion, implying that the fluid-injection-induced earthquake potential of the Gonghe EGS may be enhanced by the enrichment in laumontite over the impacts of the fluid injection operation itself. Our experimental results are of key significance in understanding instability on the laumontite-rich faults present in and transecting the Gonghe EGS reservoir. In the P-T geochemically stable domain of laumontite (<220°C), the temperature has no significant effect on its frictional strength and stability—which remains uniformly conditionally unstable. This indicates that as the depth of the geothermal reservoir increases, the frictional properties of faults will not significantly change.

The evolutionary effect-related parameter (*b* value) of our results was obtained by numerical fitting of the experimental data and we interpret this as reflecting the influence of new intergranular contacts after the reaction (Niemeijer & Spiers, 2007). Concurrently, the *b* value can also be affected by changes in porosity and uneven deformation in fault gouges (Logan et al., 1992; Marone et al., 1990). Our experimental results show that *b* increases with increasing temperature, consistent with the rate of pressure dissolution increasing and concomitantly increasing porosity during velocity steps. Hence, our results indicate an increase in the variation of frictional strength due to the evolution of the contact surface (Ikari et al., 2009; Yasuhara et al., 2003, 2005). The observations of microstructure show that local shear zones were commonly developed in our experiments (Figures S10 and S11 in Supporting Information S1).

4.2. Influence of Mineral Composition on Fault Friction

In hydrothermal environments, laumontite typically occurs together with quartz. Thus, we performed experiments with homogeneous 1:1 mixtures of laumontite/quartz under different temperature and pressure conditions ($T = 180°C$, $220°C$ and $P_f = 35$ MPa, 70 MPa). The frictional strength of the mixed gouges ($\mu = 0.74$–0.78) is less than that of pure laumontite, explained by the lower frictional coefficient of quartz gouges ($\mu = 0.6$–0.7) (Goldsby & Tullis, 2002; Logan & Rauenzahn, 1987; Lu & He, 2018; Lupini et al., 1981). Despite the overall decrease in frictional coefficient for the mixed gouge, there is no significant variation in its trend with test temperature and pressure relative to the laumontite gouge. Thus, when the laumontite content is reduced to 50% by substitution with quartz, the mixed gouge retains the same frictional instability as the pure laumontite gouge (Figure 3). Previous study shows that pure quartz exhibits velocity-strengthening phenomena within the temperature range of this study and a pore pressure of 50 MPa (Masuda et al., 2019). Therefore, this is reflected by a slightly reduced frictional strength of the mixed gouge but an unchanged range of *a–b* values—suggesting that the laumontite dominates the frictional stability response (Figures 3e, 3f, and 4).

4.3. Implications for Injection-Induced Seismicity in Gonghe Geothermal Reservoir

Logging data from the Gonghe geothermal reservoir indicate the presence of both NW- and NE-striking fractures with different permeabilities (E. Zhang et al., 2022). These fractures or faults may undergo hydrothermal alteration to varying degrees, resulting in heterogeneous precipitation on discontinuous planes. Niemeijer et al. (2010) found that ~5 wt.% layered phyllosilicates can lower the frictional strength but stabilize the faults. Although preliminary field investigations showed evidence of widespread enrichment of laumontite in the granite fractures (Figure 1), its ubiquity in the Gonghe geothermal reservoir remains unclear. Hence, an important issue is how low the enrichment level of laumontite can be but still control the frictional behavior of faults. Previous studies have shown that during the evolution of hydrothermal alteration, hydrothermal fluids can be transported through the fracture channels, microcracks, and pores, leading to the dissolution and transformation of primary minerals, as well as the precipitation of secondary minerals in various locations (Nishimoto & Yoshida, 2010). Such geochemical transformations may be further promoted or reversed by massive and long-term fluid injections for the stimulation and operation of EGS projects. Quartz, calcite, chlorite, epidote, and laumontite are common fracture-filling minerals in hydrothermally altered granites. For example, chlorite is an abundant alteration phase in both the Pohang (An et al., 2021) and Gonghe granite reservoirs (F. Zhang et al., 2023). Chlorite exhibits low frictional strength but velocity-strengthening behavior that can promote fault creep—as a low-strength but highly stable mineral. Conversely, laumontite is a high-strength but highly unstable mineral. Therefore, another open and important issue is how the contrasting and indeed opposing frictional properties of laumontite and chlorite impact the frictional strength and stability of faults containing mixtures of these (An et al., 2021; Okamoto et al., 2019).

During the Gonghe EGS stimulation, the distribution of microearthquakes (MEQs) with magnitudes larger than 0 occurred within the P-T conditions of frictional instability for laumontite (Figure 4). Although the casing toe is sealed at 3,500 m, the upward fluid migration still triggers a small number of MEQs. This is consistent with the conditionally unstable behavior of the gouge at reservoir temperatures of ~180°C—maximally conducive to the unstable slip of laumontite. This may be one of the causes for induced earthquakes caused by water injection in Gonghe EGS—the strong laumontite slips unstably and is ubiquitously unstable over the P-T range of the injection. Thus, when laumontite accumulates in geothermal reservoir faults, the risk of fault instability seems unavoidable—although maybe the sizes of patches nucleating may be limited by various methods of soft stimulation (Hofmann et al., 2018; Zang et al., 2021). Unfortunately, the absence of fluid injection above 3,500 m and below 4,000 m prevents the innate stability of laumontite in this P-T range from being examined.

Notably, our experimental results on laumontite impact the projected response of earthquakes on natural faults containing laumontite gouges. For example, seismicity on the San Andreas fault (James & Silver, 1988) and the 1995 Kobe earthquake (Tanaka et al., 2007) are potentially impacted by the role of strong velocity weakening of laumontite gouges pervasively present in the Cajon Pass area and the Nojima fault—two scientific boreholes revealed abundant laumontite in core fractures. Furthermore, the Mikabu-Northern Chichibu belt along the accretionary wedge in the subduction zone of southwestern Japan hosts hydrothermal conditions where laumontite gouges are abundant (Endo & Wallis, 2017), which may prompt the examination of the role of laumontite in the seismogenic plate boundaries.

5. Conclusions

We report for the first time the presence and frictional stability characteristics of laumontite and laumontite/quartz mixed gouges under hydrothermal conditions representative of the Gonghe EGS reservoir, China. Pure laumontite gouges are strong ($\mu = 0.73$–0.98) and the 1:1 mixture is only slightly less strong ($\mu = 0.73$–0.78), reflecting the lower frictional strength of the quartz. Strengths are constant and insensitive to temperatures (90–250°C) but increase slightly with increasing pore pressures (0–90 MPa). Stability characteristics for both pure gouge and mixtures mirror similar trends and are insensitive to fluid pressure but strongly temperature-dependent. Both pure gouge and mixtures are velocity-weakening in the range from 90°C to 220°C and maximally so at $T \sim 150$–180°C. These results with unstable sliding at $T = 90$–220°C are consistent with observed seismicity during hydraulic stimulation of the Gonghe EGS reservoir over an open-hole and uncased interval of 3,500–4,000 m. In this, MEQs are confined exclusively in the zone of frictional instability for the gouges and mixtures where the broad range of temperatures 90–220°C are those typically applicable in geothermal projects—sufficiently deep to be boiling at surface pressure but not so deep that drilling expenses increase exponentially and are prohibitive. Thus, the presence of laumontite on faults at reservoir depth is cause for consideration of the potential hazard and therefore for caution in developing the resource. Importantly, laumontite-rich gouges generally exhibit strong velocity-weakening response regardless of pore pressure, over a broad range of temperatures and are almost independent of the proportion of the coexisting mineral phase (quartz)—and thus have potential impact in anthropogenic and natural earthquakes, alike.

Data Availability Statement

The experimental data presented in this study are available in C. Zhang et al. (2023).

References

An, M., Zhang, F., Min, K. B., Elsworth, D., Marone, C., & He, C. (2021). The potential for low-grade metamorphism to facilitate fault instability in a geothermal reservoir. *Geophysical Research Letters*, *48*(11), e2021GL093552. https://doi.org/10.1029/2021GL093552

Bao, X., & Eaton, D. W. (2016). Fault activation by hydraulic fracturing in western Canada. *Science*, *354*(6318), 1406–1409. https://doi.org/10.1126/science.aag2583

Bedford, J. D., Faulkner, D. R., Allen, M. J., & Hirose, T. (2021). The stabilizing effect of high pore-fluid pressure along subduction megathrust faults: Evidence from friction experiments on accretionary sediments from the Nankai Trough. *Earth and Planetary Science Letters*, *574*, 117161. https://doi.org/10.1016/j.epsl.2021.117161

Belzer, B. D., & French, M. E. (2022). Frictional constitutive behavior of chlorite at low shearing rates and hydrothermal conditions. *Tectonophysics*, *837*, 229435. https://doi.org/10.1016/j.tecto.2022.229435

Bird, D. K., & Spieler, A. R. (2004). Epidote in geothermal systems. *Reviews in Mineralogy and Geochemistry*, *56*(1), 235–300. https://doi.org/10.2138/gsrmg.56.1.235

Blanpied, M. L., Lockner, D. A., & Byerlee, J. D. (1995). Frictional slip of granite at hydrothermal conditions. *Journal of Geophysical Research*, *100*(B7), 13045–13064. https://doi.org/10.1029/95JB00862

Chen, J., & Spiers, C. J. (2016). Rate and state frictional and healing behavior of carbonate fault gouge explained using microphysical model. *Journal of Geophysical Research: Solid Earth*, *121*(12), 8642–8665. https://doi.org/10.1002/2016JB013470

Chen, J., Verberne, B. A., & Spiers, C. J. (2015). Effects of healing on the Seismogenic potential of carbonate fault rocks: Experiments on samples from the Longmen Shan Fault, Sichuan, China. *Journal of Geophysical Research: Solid Earth*, *120*(8), 5479–5506. https://doi.org/10.1002/2015JB012051

den Hartog, S. A., Peach, C. J., de Winter, D. M., Spiers, C. J., & Shimamoto, T. (2012). Frictional properties of megathrust fault gouges at low sliding velocities: New data on effects of normal stress and temperature. *Journal of Structural Geology*, *38*, 156–171. https://doi.org/10.1016/j.jsg.2011.12.001

Dieterich, J. H. (1978). Preseismic fault slip and earthquake prediction. *Journal of Geophysical Research*, *83*(B8), 3940–3948. https://doi.org/10.1029/JB083iB08p03940

Dieterich, J. H. (1979a). Modeling of rock friction: 1. Experimental results and constitutive equations. *Journal of Geophysical Research*, *84*(B5), 2161–2168. https://doi.org/10.1029/JB084iB05p02161

Dieterich, J. H. (1979b). Modeling of rock friction: 2. Simulation of preseismic slip. *Journal of Geophysical Research*, *84*(B5), 2169–2175. https://doi.org/10.1029/JB084iB05p02169

Ellsworth, W. L. (2013). Injection-induced earthquakes. *Science*, *341*(6142), 1225942. https://doi.org/10.1126/science.1225942

Endo, S., & Wallis, S. R. (2017). Structural architecture and low-grade metamorphism of the Mikabu-Northern Chichibu accretionary wedge, SW Japan. *Journal of Metamorphic Geology*, *35*(6), 695–716. https://doi.org/10.1111/jmg.12251

Fagereng, Å., & Ikari, M. J. (2020). Low-temperature frictional characteristics of chlorite-epidote-amphibole assemblages: Implications for strength and seismic style of retrograde fault zones. *Journal of Geophysical Research: Solid Earth*, *125*(4), e2020JB019487. https://doi.org/10.1029/2020JB019487

Goldsby, D. L., & Tullis, T. E. (2002). Low frictional strength of quartz rocks at subseismic slip rates. *Geophysical Research Letters*, *29*(17), 25-1–25-4. https://doi.org/10.1029/2002GL015240

He, C., Luo, L., Hao, Q. M., & Zhou, Y. (2013). Velocity-weakening behavior of plagioclase and pyroxene gouges and stabilizing effect of small amounts of quartz under hydrothermal conditions. *Journal of Geophysical Research: Solid Earth*, *118*(7), 3408–3430. https://doi.org/10.1002/jgrb.50280

He, C., Wang, Z., & Yao, W. (2007). Frictional sliding of gabbro gouge under hydrothermal conditions. *Tectonophysics*, *445*(3–4), 353–362. https://doi.org/10.1016/j.tecto.2007.09.008

He, C., Yao, W., Wang, Z., & Zhou, Y. (2006). Strength and stability of frictional sliding of gabbro gouge at elevated temperatures. *Tectonophysics*, *427*(1–4), 217–229. https://doi.org/10.1016/j.tecto.2006.05.023

Heidari, S., Li, B., Jacquey, A. B., & Xu, B. (2023). Constitutive modeling of a laumontite-rich tight rock and the application to poromechanical analysis of deeply drilled wells. *Rock Mechanics Bulletin*, *2*(2), 100039. https://doi.org/10.1016/j.rockmb.2023.100039

Hofmann, H., Zimmermann, G., Zang, A., & Min, K.-B. (2018). Cyclic soft stimulation (CSS): A new fluid injection protocol and traffic light system to mitigate seismic risks of hydraulic stimulation treatments. *Geothermal Energy*, *6*(1), 27. https://doi.org/10.1186/s40517-018-0114-3

Hubbert, M. K., & Rubey, W. W. (1959). Role of fluid Pressure in mechanics of overthrust faulting. *Geological Society of America Bulletin*, *70*(2), 115–166. https://doi.org/10.1130/0016-7606(1959)70[115:rofpim]2.0.co;2

Igonin, N., Verdon, J. P., Kendall, J. M., & Eaton, D. W. (2021). Large-scale fracture systems are permeable pathways for fault activation during hydraulic fracturing. *Journal of Geophysical Research: Solid Earth*, *126*(3), e2020JB020311. https://doi.org/10.1029/2020JB020311

Ikari, M. J., Marone, C., & Saffer, D. M. (2011). On the relation between fault strength and frictional stability. *Geology*, *39*(1), 83–86. https://doi.org/10.1130/G31416.1

Ikari, M. J., Saffer, D. M., & Marone, C. (2009). Frictional and hydrologic properties of clay-rich fault gouge. *Journal of Geophysical Research*, *114*(B5), B05409. https://doi.org/10.1029/2008JB006089

James, E. W., & Silver, L. T. (1988). Implications of zeolites and their zonation in the Cajon pass deep drillhole. *Geophysical Research Letters*, *15*(9), 973–976. https://doi.org/10.1029/GL015i009p00973

Liou, J. G. (1971a). P-T stabilities of laumontite, Wairakite, Lawsonite, and related mineral-s in the system CaAl2Si2O8-SiO2-H2O. *Journal of Petrology*, *12*(2), 379–411. https://doi.org/10.1093/petrology/12.2.379

Liou, J. G. (1971b). Stilbite-laumontite equilibrium. *Contributions to Mineralogy and Petrology*, *31*(3), 171–177. https://doi.org/10.1007/BF00399649

Liou, J. G. (1993). Stabilities of natural epidotes. In *Proceedings of a Symposium held in Neukirchen am Großvenediger (Salzburg/Austria)* (Vol. 49, pp. 7–16).

Logan, J. M., Dengo, C. A., Higgs, N. G., & Wang, Z. Z. (1992). Fabrics of experimental fault zones: Their development and relationship to mechanical behavior. *International Geophysics*, *51*, 33–67. https://doi.org/10.1016/S0074-6142(08)62814-4

Logan, J. M., & Rauenzahn, K. A. (1987). Frictional dependence of gouge mixtures of quartz and montmorillonite on velocity, composition and fabric. *Tectonophysics*, *144*(1–3), 87–108. https://doi.org/10.1016/0040-1951(87)90010-2

Lu, Z., & He, C. (2018). Friction of foliated fault gouge with a biotite interlayer at hydrothermal conditions. *Tectonophysics*, *740*, 72–92. https://doi.org/10.1016/j.tecto.2018.05.003

Lupini, J. F., Skinner, A. E., & Vaughan, P. R. (1981). The drained residual strength of cohesive soils. *Géotechnique*, *31*(2), 181–213. https://doi.org/10.1680/geot.1981.31.2.181

Majer, E. L., Baria, R., Stark, M., Oates, S., Bommer, J., Smith, B., & Asanuma, H. (2007). Induced seismicity associated with enhanced geothermal systems. *Geothermics*, *36*(3), 185–222. https://doi.org/10.1016/j.geothermics.2007.03.003

Marone, C. (1998). Laboratory-derived friction laws and their application to seismic faulting. *Annual Review of Earth and Planetary Sciences*, *26*(1), 643–696. https://doi.org/10.1146/annurev.earth.26.1.643

Marone, C., & Kilgore, B. (1993). Scaling of the critical slip distance for seismic faulting with shear strain in fault zones. *Nature*, *362*(6421), 618–621. https://doi.org/10.1038/362618a0

Marone, C., Raleigh, C. B., & Scholz, C. H. (1990). Frictional behavior and constitutive modeling of simulated fault gouge. *Journal of Geophysical Research*, *95*(B5), 7007–7025. https://doi.org/10.1029/JB095iB05p07007

Masuda, K., Arai, T., & Takahashi, M. (2019). Effects of frictional properties of quartz and feldspar in the crust on the depth extent of the seismogenic zone. *Progress in Earth and Planetary Science*, *6*(1), 50. https://doi.org/10.1186/s40645-019-0299-5

Morrow, C. A., & Byerlee, J. D. (1991). A note on the frictional strength of laumontite from Cajon Pass, California. *Geophysical Research Letters*, *18*(2), 211–214. https://doi.org/10.1029/91GL00209

Morrow, C. A., Moore, D. E., & Lockner, D. A. (2000). The effect of mineral bond strength and adsorbed water on fault gouge frictional strength. *Geophysical Research Letters*, *27*(6), 815–818. https://doi.org/10.1029/1999GL008401

Niemeijer, A., Marone, C., & Elsworth, D. (2010). Fabric induced weakness of tectonic faults. *Geophysical Research Letters*, *37*(3), L03304. https://doi.org/10.1029/2009GL041689

Niemeijer, A. R., & Collettini, C. (2014). Frictional properties of a low-angle normal fault under in situ conditions: Thermally-activated velocity weakening. *Pure and Applied Geophysics*, *171*(10), 2641–2664. https://doi.org/10.1007/s00024-013-0759-6

Niemeijer, A. R., & Spiers, C. J. (2007). A microphysical model for strong velocity weakening in phyllosilicate-bearing fault gouges. *Journal of Geophysical Research*, *112*(B10), B10405. https://doi.org/10.1029/2007JB005008

Nishimoto, S., & Yoshida, H. (2010). Hydrothermal alteration of deep fractured granite: Effects of dissolution and precipitation. *Lithos*, *115*(1–4), 153–162. https://doi.org/10.1016/j.lithos.2009.11.015

Okamoto, A. S., Niemeijer, A. R., Takeshita, T., Verberne, B. A., & Spiers, C. J. (2020). Frictional properties of actinolite-chlorite gouge at hydrothermal conditions. *Tectonophysics*, *779*, 228377. https://doi.org/10.1016/j.tecto.2020.228377

Okamoto, A. S., Verberne, B. A., Niemeijer, A. R., Takahashi, M., Shimizu, I., Ueda, T., & Spiers, C. J. (2019). Frictional properties of simulated chlorite gouge at hydrothermal conditions: Implications for subduction megathrusts. *Journal of Geophysical Research: Solid Earth*, *124*(5), 4545–4565. https://doi.org/10.1029/2018JB017205

Prante, M. R., & Evans, J. P. (2015). Pseudotachylyte and fluid alteration at seismogenic depths (Glacier Lakes and Granite Pass Faults, Central Sierra Nevada, USA). *Pure and Applied Geophysics*, *172*(5), 1203–1227. https://doi.org/10.1007/s00024-014-0989-2

Rice, J. R. (1983). Constitutive relations for fault slip and earthquake instabilities. *Pure and Applied Geophysics*, *121*(3), 443–475. https://doi.org/10.1007/BF02590151

Ruina, A. (1983). Slip instability and state variable friction laws. *Journal of Geophysical Research*, *88*(B12), 10359–10370. https://doi.org/10.1029/JB088iB12p10359

Scholz, C. (1998). Earthquakes and friction laws. *Nature*, *391*(6662), 37–42. https://doi.org/10.1038/34097

Schultz, R., Atkinson, G., Eaton, D. W., Gu, Y. J., & Kao, H. (2018). Hydraulic fracturing volume is associated with induced earthquake productivity in the Duvernay play. *Science*, *359*(6373), 304–308. https://doi.org/10.1126/science.aao0159

Shimamoto, T., & Logan, J. M. (1981). Effects of simulated clay gouges on the sliding behavior of Tennessee sandstone. *Tectonophysics*, *75*(3–4), 243–255. https://doi.org/10.1016/0040-1951(81)90276-6

Smith, S. A. F., Tesei, T., Scott, J. M., & Collettini, C. (2017). Reactivation of normal faults as high-angle reverse faults due to low frictional strength: Experimental data from the Moonlight Fault Zone, New Zealand. *Journal of Structural Geology*, *105*, 34–43. https://doi.org/10.1016/j.jsg.2017.10.009

Tanaka, H., Omura, K., Matsuda, T., Ikeda, R., Kobayashi, K., Murakami, M., & Shimada, K. (2007). Architectural evolution of the Nojima fault and identification of the activated slip layer by Kobe earthquake. *Journal of Geophysical Research*, *112*(B7), B07304. https://doi.org/10.1029/2005JB003977

Yasuhara, H., Elsworth, D., & Polak, A. (2003). A mechanistic model for compaction of granular aggregates moderated by pressure solution. *Journal of Geophysical Research*, *108*(B11), 2530. https://doi.org/10.1029/2003JB002536

Yasuhara, H., Marone, C., & Elsworth, D. (2005). Fault zone restrengthening and frictional healing: The role of pressure solution. *Journal of Geophysical Research*, *110*(B6), B06310. https://doi.org/10.1029/2004JB003327

Zang, A., Zimmermann, G., Hofmann, H., Niemz, P., Kim, K. Y., Diaz, M., et al. (2021). Relaxation damage control via fatigue-hydraulic fracturing in granitic rock as inferred from laboratory-mine-and field-scale experiments. *Scientific Reports*, *11*(1), 6780. https://doi.org/10.1038/s41598-021-86094-5

Zhang, C., Fan, D., Elsworth, D., He, M., Zhao, X., Zhu, C., & Zhang, H. (2024). Mechanisms of stress-and fluid-pressure-driven fault reactivation in Gonghe granite: Implications for injection-induced earthquakes. *International Journal of Rock Mechanics and Mining Sciences*, *174*, 105642. https://doi.org/10.1016/j.ijrmms.2024.105642

Zhang, C., Hu, Z., Derek, E., Zhang, L., He, M., He, C., & Yao, L. (2023). Shear experiment data for laumontite and mixed gouges at different temperatures and pore pressures [Dataset]. *Dryad*. https://doi.org/10.5061/dryad.9zw3r22kf

Zhang, E., Wen, D. g., Wang, G. l., Yan, W. d., Wang, W. s., Ye, C. m., et al. (2022). The first power generation test of hot dry rock resources exploration and production demonstration project in the Gonghe Basin, Qinghai Province, China. *China Geology*, *5*(3), 372–382. https://doi.org/10.31035/cg2022038

Zhang, F., Cao, S., An, M., Zhang, C., & Derek, E. (2023). Friction and stability of granite faults in the Gonghe geothermal reservoir and implications for injection-induced seismicity. *Geothermics*, *112*, 102730. https://doi.org/10.1016/j.geothermics.2023.102730

Zhang, S., Yan, W., Dunpeng, L., Jia, X., Zhang, S., Shengtao, L., et al. (2018). Characteristics of geothermal geology of the Qiabuqia HDR in Gonghe Basin, Qinghai Province. *Geology in China*, *45*(6), 1087–1102. (in Chinese with English abstract).